0026-895X/10/7806-1088–1095$20.00
MOLECULAR PHARMACOLOGY
Vol. 78, No. 6
66100/3644098
Mol Pharmacol 78:1088–1095, 2010
Printed in U.S.A.

The Specific Slow Afterhyperpolarization Inhibitor UCL2077 Is a Subtype-Selective Blocker of the Epilepsy Associated KCNQ Channels[S]

Heun Soh and Anastassios V. Tzingounis

Department of Physiology and Neurobiology, University of Connecticut, Storrs, Connecticut

Received May 5, 2010; accepted September 14, 2010

ABSTRACT

Mutations in members of the KCNQ channel family underlie multiple diseases affecting the nervous and cardiovascular systems. Despite their clinical relevance, research into these channels is limited by the lack of subtype-selective inhibitors, making it difficult to differentiate the physiological function of each family member in vivo. We have proposed that KCNQ channels might partially underlie the calcium-activated slow afterhyperpolarization (sAHP), a neuronal conductance whose molecular components are uncertain. Here, we investigated whether 3-(triphenylmethylaminomethyl)pyridine (UCL2077), identified previously as an inhibitor of the sAHP in neurons, acts on members of the KCNQ family expressed in heterologous cells. We found that 3 μM UCL2077 strongly inhibits KCNQ1 and KCNQ2 channels and weakly blocks KCNQ4 channels in a voltage-independent manner. In contrast, UCL2077 potentiates KCNQ5 channels at more positive membrane potentials, with little effect at negative membrane potentials. We found that the effect of UCL2077 on KCNQ3 is bimodal: currents are enhanced at negative membrane potentials and inhibited at positive potentials. We found that UCL2077 facilitates KCNQ3 currents by inducing a leftward shift in the KCNQ3 voltage-dependence, a shift dependent on tryptophan 265. Finally, we show that UCL2077 has intermediate effects on KCNQ2/3 heteromeric channels compared with KCNQ2 and KCNQ3 homomers. Together, our data demonstrate that UCL2077 acts on KCNQ channels in a subtype-selective manner. This feature should make UCL2077 a useful tool for distinguishing KCNQ1 and KCNQ2 from less-sensitive KCNQ family members in neurons and cardiac cells in future studies.

Introduction

The KCNQ channel family includes five genes, known as *Kcnq1-5* (Jentsch, 2000). Most family members are required for proper function of either the nervous or cardiovascular system, depending on their specific localization pattern. Loss of function mutations in *Kcnq1* lead to long QT syndrome, a heart disorder, as well as a congenital form of deafness (Wollnik et al., 1997; van den Berg et al., 1997). KCNQ1 channels were also recently implicated in sudden unexplained death in epilepsy (Goldman et al., 2009). Mutations in *Kcnq2* and *Kcnq3* underlie a rare form of pediatric epilepsy, benign familial neonatal convulsions (Biervert et al., 1998; Charlier et al., 1998; Singh et al., 1998), whereas KCNQ4 loss-of-function mutations lead to nonsyndromic sensorineural deafness type 2, a form of progressive hearing loss (Kubisch et al., 1999). KCNQ5 is also expressed in the nervous system but is not yet associated with any neurological disorders (Lerche et al., 2000; Schroeder et al., 2000).

Given their obvious physiological importance, it is not surprising that small-molecule compounds that target KCNQs are believed to hold great therapeutic promise. Retigabine, a KCNQ channel potentiator, has been successfully used for the treatment of pharmacoresistant epilepsy in phase III clinical trials (Maljevic et al., 2010). Other KCNQ channel modulators have been proposed for the treatment of ischemia, stroke, and migraines (Wua and Dworetzky, 2005; Maljevic et al., 2008). However, none of the KCNQ inhibitors described to date act exclusively on specific KCNQ family members, although compounds targeting specific KCNQ populations are likely to be advantageous either as cognitive enhancers or for the treatment of disease.

A subunit-specific KCNQ inhibitor could also be used to probe the contribution of each KCNQ channel subunit to physiological processes in the nervous system. Currently KCNQ-mediated currents are isolated by linopirdine or

This research was supported by the National Institutes of Health National Institute of Neurological Disorders and Stroke [Grant NS060890].

Article, publication date, and citation information can be found at http://molpharm.aspetjournals.org.

doi:10.1124/mol.110.066100.

[S] The online version of this article (available at http://molpharm.aspetjournals.org) contains supplemental material.

ABBREVIATIONS: sAHP, slow afterhyperpolization; EGFP, enhanced green fluorescence protein; HEK, human embryonic kidney; UCL2077, 3-(triphenylmethylaminomethyl)pyridine; XE-991, 10,10-bis(4-pyridinylmethyl)-9(10*H*)-anthracenone; G-V, conductance-to-voltage.

10,10-bis(4-pyridinylmethyl)-9(10*H*)-anthracenone (XE-991), two nonselective KCNQ channel blockers (Wang et al., 1998). Using these blockers, investigators demonstrated that KCNQ channels mediate the M-current, a voltage-activated potassium conductance found in most neurons. In the absence of subunit-selective drugs, knockout mice and loss-of-function mice have been used to understand the contribution of each KCNQ subunit (Peters et al., 2005; Kharkovets et al., 2006; Otto et al., 2006; Singh et al., 2008; Tzingounis and Nicoll, 2008; Tzingounis et al., 2010), although these mice may exhibit developmental compensation or homeostatic changes.

We have proposed that KCNQ2, -3, and -5 channels may contribute to the slow afterhyperpolarization (sAHP), a calcium-activated potassium conductance that limits neuronal firing (Nicoll, 1988; Tzingounis and Nicoll, 2008; Tzingounis et al., 2010). To corroborate our previous findings, we decided to test whether the small molecule 3-(triphenylmethyaminmomethyl) pyridine (UCL2077) acts on KCNQ channels. Shah et al. (2006) first identified UCL2077 as a selective blocker of the sAHP in rat CA1 neurons, although they did not know its molecular target. Later studies demonstrated that UCL2077 blocked the sAHP generated after activation of L-type calcium channels in thalamic neurons (Zhang et al., 2009) and the sAHP in gonadotropin-releasing hormone neurons (Lee et al., 2010). Thus, based on our hypothesis that KCNQ channels contribute to the sAHP, we predicted that UCL2077 might modulate KCNQ channels.

In this study, we characterized the effects of UCL2077 on all members of the KCNQ channel family in heterologous cells. We report that UCL2077 is a potent inhibitor only for KCNQ1 and KCNQ2 channels. It modestly inhibits KCNQ4 channels and potentiates KCNQ5-mediated currents in a voltage-dependent manner. The effects of UCL2077 on KCNQ3 are more complicated, either facilitating or inhibiting depending on the membrane potential. We found that KCNQ3 facilitation depends on tryptophan 265, an amino acid implicated previously in the agonist activity of retigabine (Schenzer et al., 2005). Our study thus identifies UCL2077 as the first subtype-selective inhibitor of KCNQ channels. In future studies, UCL2077 could be used to discriminate the effects of KCNQ1 and KCNQ2 from other KCNQ family members in the heart and brain.

Materials and Methods

Materials. Chemicals and reagents were obtained from Sigma-Aldrich (St. Louis, MO). XE-991 was acquired from Ascent Scientific (Avonmouth, Bristol, UK), and Dulbecco's modified Eagle's medium, minimal essential medium, penicillin/streptomycin, and fetal calf serum were purchased from Invitrogen (Carlsbad, CA).

Recordings in Hippocampal Slices. Experiments were carried out according to the guidelines of the University of Connecticut–Storrs Institutional Animal Care and Use Committee. Transverse hippocampal slices (300 μm) were prepared from 10- to 16-day-old C57/Bl6 mice. After animals were deeply anesthetized with isoflurane (Baxter Healthcare Corp., McGaw Park, IL), they were rapidly decapitated, and the hippocampus was dissected out and sliced with a vibratome Microm HM 650V (Thermo Fisher Scientific, Waltham, MA). The hippocampus was cut in a cold solution containing 25 mM $NaHCO_3$, 200 mM sucrose, 10 mM glucose, 2.5 mM KCl, 1.3 mM NaH_2PO_4, 0.5 mM $CaCl_2$, and 7 mM $MgCl_2$. Slices were incubated at 35°C for 30 min in the cutting solution, then moved to room temperature for 1 h, and finally stored at room temperature in the extracellular recording solution 119 mM NaCl, 2.5 mM KCl, 1.3 mM $MgSO_4$, 2.5 mM $CaCl_2$, 1 mM NaH_2PO_4, 26 mM $NaHCO_3$, and 10 mM glucose, equilibrated with 95% O_2/5% CO_2. All experiments were performed at room temperature. Whole-cell current-clamp recordings were obtained using borosilicate glass electrodes having resistances of 4 to 6 MΩ (World Precision Instruments, Inc., Sarasota, FL). Pyramidal cells from either the CA1 or CA3 area of the hippocampus were visually identified with infrared differential interference contrast optics using a 40× water-immersion objective lens on an upright microscope (Olympus BX51; Olympus, Tokyo, Japan). The internal recording solution consisted of the following): 130 mM potassium methylsulfate, 10 mM KCl, 10 mM HEPES, 20 mM *myo*-inositol, 4 mM NaCl, 4 mM Mg_2ATP, and 0.4 mM Na_4GTP (osmolarity, 300–305 mOsM). The pH was adjusted to 7.25 to 7.3 with KOH. The methylsulfate anion was used to obtain stable sAHP recordings (Zhang et al., 1994). Current-clamp recordings were performed using a Multiclamp 700B amplifier set in bridge mode (Molecular Devices, Sunnyvale, CA), low pass-filtered at 2 kHz, sampled at 10 kHz, and analyzed offline using Axograph X (Axograph Scientific, Sydney, Australia) and Kaleidagraph (Synergy Software, Reading, PA). Neurons were held at −60 mV. To avoid significant drift of the membrane potential during the course of the experiment, we manually applied a small DC current to maintain the membrane potential at approximately −60 mV, never allowing it to fluctuate for more than ±3 mV. To elicit the sAHP, we depolarized cells by injecting 1 nA current for 100 (CA3) or 300 ms (CA1) at 60-s intervals. To quantify the sAHP, we integrated the response for 18 s starting 1 s after the current injection step. The effects of UCL2077 were expressed as the percentage of inhibition relative to the response before UCL2077 application in the same cell.

Recordings in HEK293T and Chinese Hamster Ovary Cells. HEK293T cells were transfected with recombinant DNA (0.5–5 μg) using Lipofectamine 2000 (Invitrogen) and recorded 24 to 72 h after transfection. For KCNQ1 only, we used Chinese hamster ovary cells instead of HEK293T cells. All experiments were performed at room temperature. To minimize rundown, KCNQ-mediated currents were recorded using the perforated-patch recording technique for all cells except for those expressing either KCNQ4 or KCNQ5, which were recorded with conventional whole-cell patch-clamp recordings because of their relatively stable currents. The recording electrodes were filled with solution containing 112 mM potassium gluconate, 10 mM KCl, 20 mM KOH, 4 mM magnesium·ATP, 4.976 mM $CaCl_2$, 20 mM HEPES, and 10 EGTA · KOH, pH 7.2. For perforated-patch recordings, 300 to 400 μg/ml amphotericin B (Sigma-Aldrich) was added to the internal solution. The electrode resistances were 2 to 4 MΩ. The extracellular solution contained 144 mM NaCl, 2.5 mM KCl, 2.25 mM $CaCl_2$, 1.2 mM $MgCl_2$, 10 mM HEPES, and 22 mM D-glucose, pH 7.2. Voltage pulses were applied at 10-s intervals from a holding potential of −70 mV to various test pulses and returned to −55 mV as described in the figure legends. The data were low pass-filtered at 2 kHz and sampled at 10 kHz. For all recordings, we used a Multiclamp 700B amplifier interfaced to a computer through a Digidata 1440A digitizer (Molecular Devices). Data were acquired with Clampex version 10.2 (Molecular Devices) and analyzed offline using Clampfit version 10.2 (Molecular Devices) and Origin version 8 (OriginLab Corp, Northampton, MA).

Molecular Biology. *mKcnq*1 (GenBank accession number BC055304), *hKcnq*2 (GenBank accession number AF110020), and *hKcnq*5 (GenBank accession number BC117359) were obtained from Open Biosystems (Huntsville, AL) and were subcloned into a pIRES2-DsRed-Express vector (Clontech, Mountain View, CA). *hKcnq*3 (generous gift of Dr. T. J. Jentsch) was subcloned into pIRES2-EGFP (Clontech). Site-directed mutagenesis was performed using the QuikChange II mutagenesis kit (Stratagene, La Jolla, CA) to generate $hKcnq3^{A315T}$ and $hKcnq3^{W265L/A315T}$ channels, and the mutations were validated by DNA sequencing. *hKcnq4* in the pcDNA3 vector was the generous gift of Dr. M.S. Shapiro. To identify

cells expressing *hKcnq4*, this construct was cotransfected with an EGFP-pCMV vector. For coexpression experiments of KCNQ2 and KCNQ3, we used the *mKcnq*2-IRES-*rKcnq*3 construct kindly provided by Dr. I. B. Levitan (Wen and Levitan, 2002).

Analysis. The conductance-to-voltage relationships for channel activation were determined from measurements of tail current amplitudes at −55 mV. The data were fitted with a single Boltzmann equation of the form $G = G_{max}/(1 + e^{(V0.5 - V)/k})$, where G is the tail current amplitude at −55 mV, $V_{0.5}$ is the voltage producing half-maximal activation, k is the slope factor, and G_{max} refers to the maximal conductance.

The concentration-inhibition curve is plotted as the fractional current remaining ($I_{normalized}$) after application of different UCL2077 concentrations. The concentration-inhibition curve was fitted by the Hill equation having the form $I_{normalized} = I_1 + (I_2 - I_1) \times [UCL2077]^{nH}/([UCL2077]^{nH} - IC_{50}{}^{nH})$. I_1 is the normalized current before application of UCL2077 constrained to 1 (i.e., no block), I_2 is the maximum current blocked constrained to 0 (i.e., 100% block), [UCL2077] refers to concentration of UCL2077, IC_{50} is the UCL2077 concentration producing 50% of the maximum response, and n_H is the Hill coefficient. The concentration-inhibition plot was measured at 0 mV. Because of the incomplete block of KCNQ3, we obtained values for KCNQ3 by constraining n_H to a value of 2, similar to the KCNQ2 value.

Group data are presented as mean ± S.E., and statistical tests were performed using paired Student's t tests. A value giving $p < 0.05$ was considered to be significant.

Results

UCL2077 Modulates KCNQ1–5 Channels in a Subtype-Selective Manner. We have proposed that KCNQ channels may contribute to the calcium-activated sAHP in a cell type-specific manner based on data from KCNQ knockout and knock-in mice (Tzingounis and Nicoll, 2008; Tzingounis et al., 2010). A prediction of this hypothesis is that compounds that modulate the sAHP should also modulate KCNQ channels. One such compound, UCL2077 was reported to partially block the sAHP in hippocampal, thalamic, and hypothalamic neurons (Shah et al., 2006; Zhang et al., 2009; Lee et al., 2010). We first verified the activity of UCL2077 by recording the effect of 10 μM UCL2077, a concentration shown previously to inhibit the sAHP in brain slices (Shah et al., 2006; Zhang et al., 2009; Lee et al., 2010) on neurons in mouse hippocampal slices (Fig. 1). We found that UCL2077 blocked the CA1 sAHP by 49 ± 11% ($n = 6$) and the CA3 sAHP by 47 ± 8% ($n = 5$), similar to the percentage of inhibition described previously.

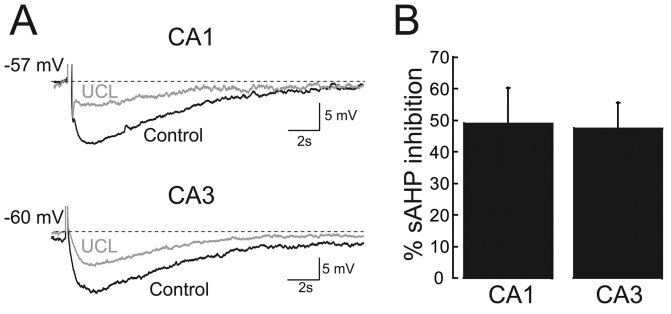

Fig. 1. UCL2077 inhibits the sAHP in mouse hippocampus. A, top, representative sAHP recording from a CA1 pyramidal neuron induced by a 300 ms, 1 nA current pulse before (black) and after (gray) application of 10 μM UCL2077. Bottom, representative sAHP recording from a CA3 pyramidal neuron induced by a 100-ms, 1-nA current pulse before (black) and after (gray) application of 10 μM UCL2077. B, graph summarizing the sAHP block induced by 10 μM UCL2077.

We next determined whether UCL2077 modulates KCNQ channels by characterizing its effects on KCNQ1–5 homomeric channels expressed in heterologous cells. Cells expressing KCNQ1–5 channels showed robust voltage- and time-dependent currents characteristic of KCNQ-mediated events (Fig. 2). Upon application of 3 μM UCL2077, a concentration previously used to study potassium channels in heterologous cells (Shah et al., 2006), we observed that the responses of KCNQ channels varied depending on the subtype. In particular, UCL2077 almost completely blocked KCNQ1 currents (97 ± 4% at 0 mV, $n = 3$) and strongly attenuated KCNQ2 currents (76 ± 4% at 0 mV, $n = 6$) (Fig. 2). Inspection of the normalized current-to-voltage relationship (I-V) collected from several independent experiments indicated that UCL2077 inhibits KCNQ1- and KCNQ2-mediated currents across all membrane potentials (Fig. 2). In contrast to KCNQ1 and KCNQ2, KCNQ3 currents are nearly insensitive to 3 μM UCL2077 (13 ± 4% blocked at 0 mV, $n = 7$), and KCNQ4 is only weakly sensitive (36 ± 10% blocked at 0 mV, $n = 6$) (Fig. 2). In addition, we observed that application of UCL2077 consistently increased KCNQ5 currents at 0 mV by 30 ± 12% ($n = 6$). Potentiation could be seen only at positive membrane potentials (Fig. 2). Together, our data indicated that UCL2077 primarily blocks KCNQ1 and KCNQ2 channels and is therefore a subtype-selective KCNQ channel inhibitor.

UCL2077 Shifts the Voltage-Dependence of Activation for Select KCNQ Subtypes. Many KCNQ channel modulators exert their effects in part by changing the voltage-dependence of channel activation. To further probe the effects of UCL2077, we measured the conductance-to-voltage (G-V) relationship for KCNQ2–5 channels. We could not obtain a G-V relationship for KCNQ1 channels because of the complete block by UCL2077. As we observed for current inhibition, we found that the effects of UCL2077 on the normalized G-V relationships varied by channel subtype.

KCNQ2 channels did not exhibit any significant changes in their G-V relationship (control $V_{0.5} = -29.7 \pm 1.5$ mV; UCL2077 $V_{0.5} = -26 \pm 3.2$ mV, $n = 6$; $p = 0.21$) (Fig. 3A). UCL2077 induced a rightward shift in the KCNQ4 G-V relationship, such that channel activation required more depolarized values. The half-activation voltage of KCNQ4 was 7.6 ± 3.1 mV before and 20.7 ± 5.2 mV after UCL2077 application ($n = 6$, $p < 0.05$) (Fig. 3C), and this is likely to contribute to KCNQ4 inhibition at 0 mV (Fig. 2). There was also a decrease to the G_{max} (18.8 ± 3.7%, $n = 6$; $p < 0.05$). UCL2077 induced a rightward shift of the KCNQ5 G-V to more depolarized potentials (control $V_{0.5} = -43.1 \pm 1.5$ mV, UCL2077 $V_{0.5} = -38.6 \pm 2.6$ mV, $n = 6$, $p < 0.01$), a change that could counteract its facilitatory effect at 0 mV. Because of the KCNQ5 conductance decrease at positive membrane potentials, we could not accurately determine the KCNQ5 G_{max}.

We also observed that UCL2077 shifted the G-V relationship leftward for KCNQ3 channels, an effect most apparent at hyperpolarized membrane potentials (control $V_{0.5} = -42.7 \pm 0.8$ mV; UCL2077 $V_{0.5} = -48.8 \pm 2.0$ mV, $n = 7$; $p < 0.01$) (Fig. 3B). This leftward shift was unexpected given the apparent insensitivity of KCNQ3 channels to UCL2077 at 0 mV. We therefore more closely examined KCNQ3 currents in

the presence and absence of UCL2077 and found that UCL2077 actually had a bimodal effect on KCNQ3 channels. Although it had little effect at 0 mV, UCL2077 potentiated KCNQ3 channels at hyperpolarized potentials and inhibited the channels at more depolarized potentials (Fig. 3B, inset). This small facilitation is difficult to observe in the normalized I-V curve (Fig. 2) because of the small size of the currents at hyperpolarized potentials smaller than −50 mV. We were intrigued by this bimodal activity, unique to KCNQ3, and investigated it further.

Tryptophan 265 Is Critical for UCL2077 Potentiation of KCNQ3. The bimodal action of UCL2077 on KCNQ3 channels was reminiscent of behavior reported previously for retigabine, a KCNQ channel and M-current potentiator. Retigabine is usually described as a channel potentiator because it induces a leftward shift in the half-activation potential, thus facilitating KCNQ currents measured at hyperpolarized membrane potentials. However, what is less known is that retigabine inhibits the M-current at membrane potentials positive to −10 mV (Tatulian et al., 2001). We therefore questioned whether UCL2077 might interact with similar amino acid residues on KCNQ3 as retigabine.

Previous studies have identified tryptophan 265 (Trp265), a residue within the cytoplasmic region of the S5 α helix, as a critical amino acid for the binding of retigabine to KCNQ3 channels (Schenzer et al., 2005). To examine whether the UCL2077 also mediates its effect through Trp265, we replaced the tryptophan with a leucine (W265L). However, the KCNQ3^{W265L} channels (W265L) expressed poorly in HEK293T cells and exhibited very small currents. To overcome this complication, we engineered a different mutation to produce KCNQ3^{A315T} channels (A315T). It has been shown previously that A315T channels retain all known voltage-dependent properties of wild-type KCNQ3 channels but have a much higher potassium flux and thus give rise to larger currents (Zaika et al., 2008). The large current responses in A315T channels made it possible to more clearly observe the effects of UCL2077 at the hyperpolarized voltage range. Similar to KCNQ3 wild-type channels, UCL2077 blocked the A315T channels at more positive potentials and facilitated the channels at more negative potentials (Fig. 4A$_1$) and induced a leftward shift in the voltage-dependence ($V_{0.5}$ = −25.1 ± 2.9 mV before and −32.9 ± 3.1 mV after UCL2077, n = 8, $p<0.001$) (Fig. 4A$_2$).

After verifying the effects of UCL2077 on A315T, we generated channels with both the W265L and A315T mutations (W265L/A315T). In contrast to A315T, UCL2077 did not facilitate W265L/A315T-containing channels at any membrane

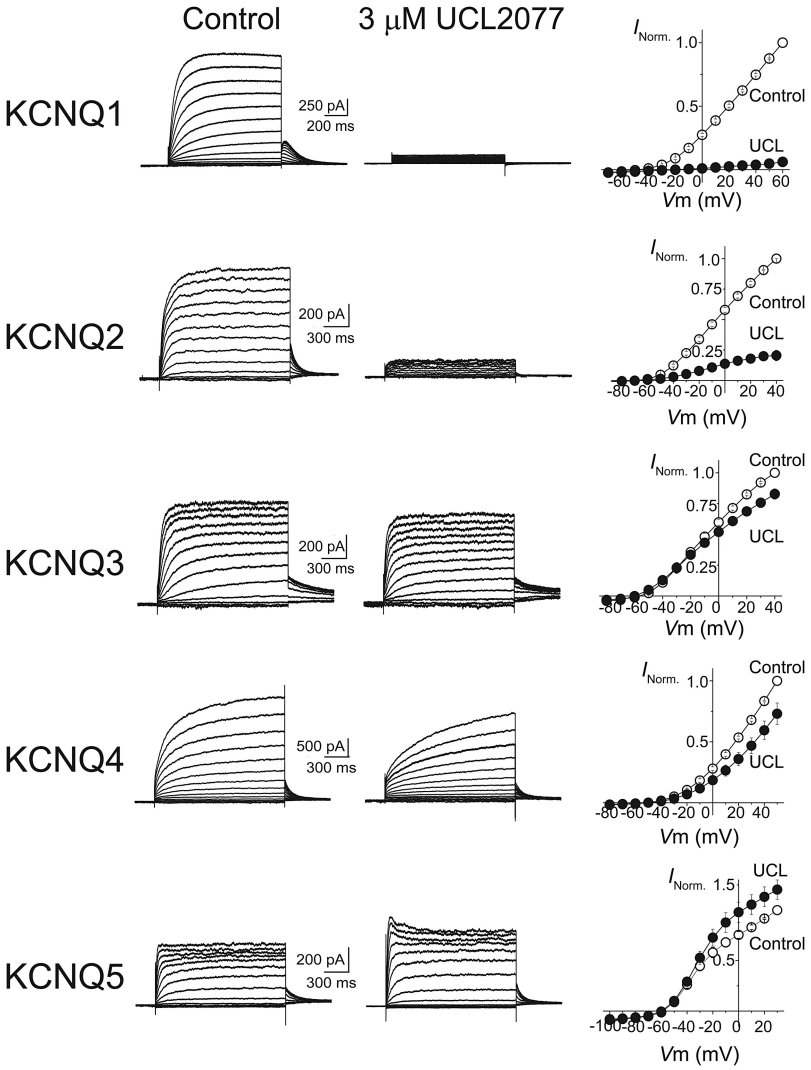

Fig. 2. UCL2077 modulates KCNQ channels in a subtype-selective manner. Left and middle, representative current traces at different membrane potentials from heterologous cells expressing KCNQ1, KCNQ2, KCNQ3, KCNQ4, or KCNQ5 before (left) and after (middle) application of 3 μM UCL2077. Right, current-to-voltage relationships for each KCNQ subunit are shown. Normalized current values were plotted against test potentials before (○) and after (●) the addition of 3 μM UCL2077. For these experiments, KCNQ currents were measured at various test potentials elicited by a short (1–1.5 s) depolarization from −70 mV and were followed by a return step to −55 mV. Test potentials were at 10-mV increments with the following ranges: KCNQ1, −70 to +60 mV; KCNQ2 and KCNQ3, −80 to +40 mV, KCNQ4, −80 to +50 mV, and KCNQ5, −100 to +30 mV.

potential tested and instead inhibited channels at all potentials (Fig. 4B$_1$). Likewise, it did not induce a shift in the voltage-dependence of activation (Fig. 4B$_2$). Together, our data indicate that similar to retigabine, facilitation by UCL2077 requires Trp265.

UCL2077 Has a Lower Affinity for KCNQ3 than KCNQ2. For the remainder of our study, we decided to examine the effects of UCL2077 on KCNQ2 and KCNQ3 in more detail. We chose these channels because they are ubiquitously expressed throughout the nervous system, and KCNQ2/3 heteromeric channels are believed to underlie the M-current (Wang et al., 1998; Jentsch, 2000). Furthermore, our initial set of experiments suggested that KCNQ2 and KCNQ3 are affected quite differently by UCL2077.

To examine the dose-dependent block of KCNQ2 currents at 0 mV, we determined the magnitude of KCNQ2 inhibition by different UCL2077 concentrations (Fig. 5, A and C). The inhibition of KCNQ2 reversed upon UCL2077 washout, and we observed a small rebound above the baseline level in some

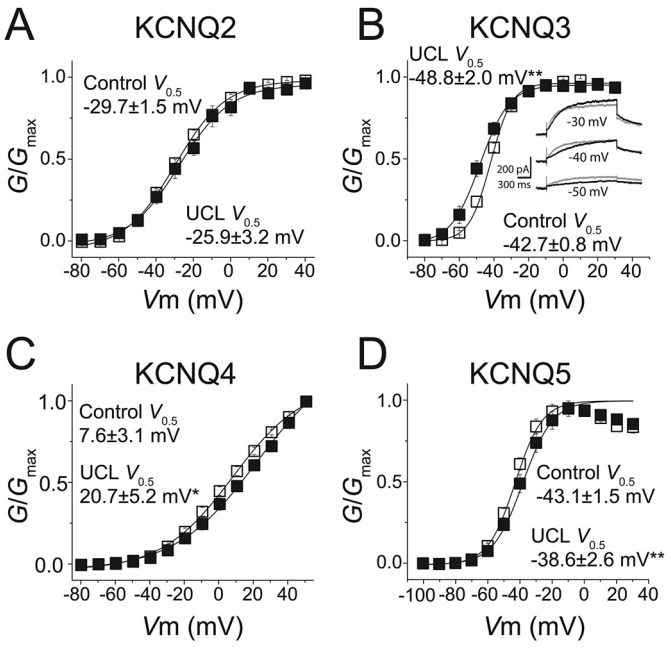

Fig. 3. UCL2077 differentially alters the conductance-to-voltage relationships of KCNQ channels. Conductance-to-voltage relationship for KCNQ2 (A; $n = 6$), KCNQ3 (B; $n = 7$), KCNQ4 (C; $n = 6$), and KCNQ5 (D, $n = 6$) were obtained from tail currents at −55 mV in the presence (■) and absence (□) of 3 μM UCL2077. B, inset, representative KCNQ3 currents at −50, −40, or −30 mV test potentials in the absence (black) and presence (gray) of 3 μM UCL2077. *, $p < 0.05$, **, $p < 0.01$.

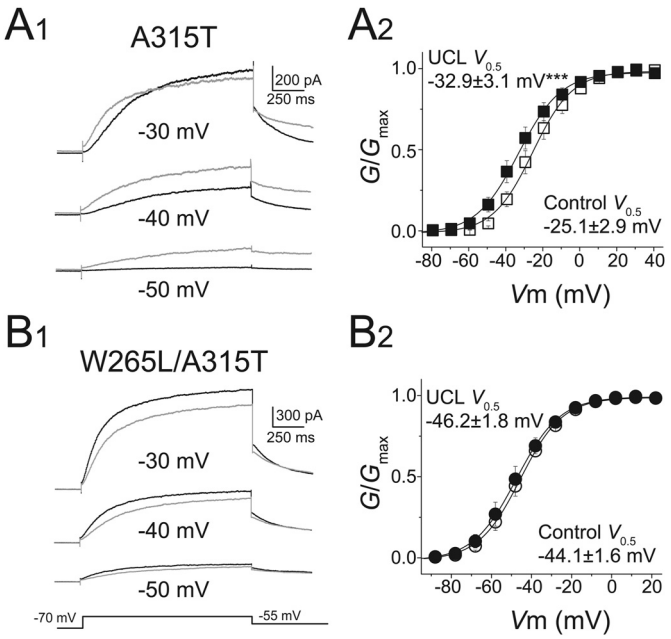

Fig. 4. Tryptophan 265 is critical for UCL2077 potentiation of KCNQ3. A$_1$, representative KCNQ3^{A315T} currents elicited by the indicated voltages before (black) and after (gray) application of 3 μM UCL2077. A$_2$, conductance-to-voltage relationship of KCNQ3^{A315T} currents in the presence (■) and absence (□) of 3 μM UCL2077 ($n = 8$). B$_1$, representative KCNQ3$^{W265L/A315T}$ currents elicited by the indicated voltages before (black) and after (gray) application of 3 μM UCL2077. B$_2$, conductance-to-voltage relationship of KCNQ3$^{W265L/A315T}$ currents in the presence (■) and absence (□) of 3 μM UCL2077 ($n = 5$). ***, $p < 0.001$.

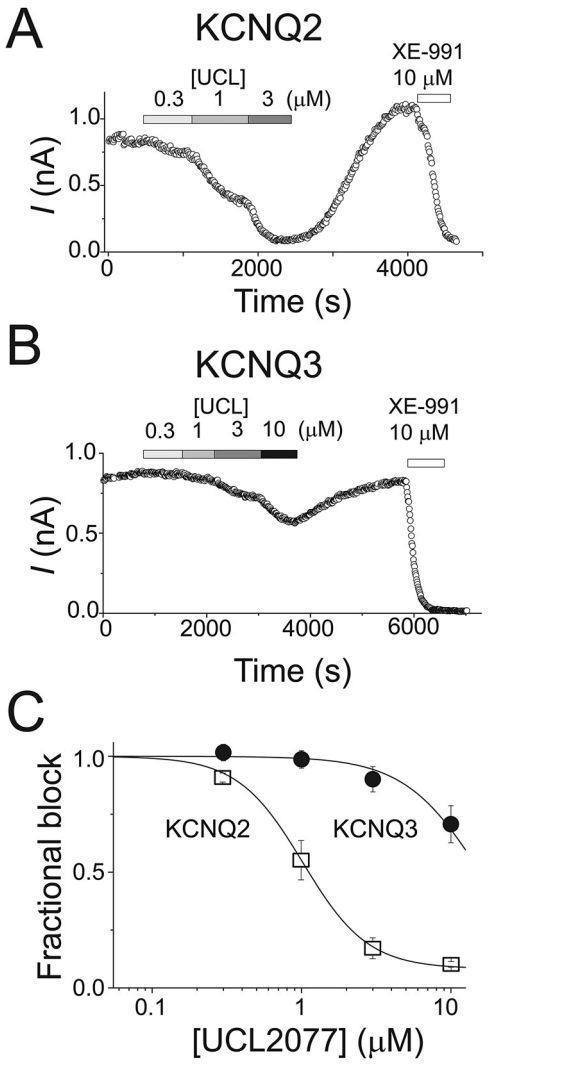

Fig. 5. UCL2077 has a higher affinity for KCNQ2 channels than KCNQ3 channels. Representative time course of KCNQ2 (A) and KCNQ3 (B) currents at a test potential of 0 mV in the presence of the indicated compounds. Currents were elicited every 10 s. C, concentration-dependence of UCL2077 inhibition of KCNQ2 and KCNQ3 currents. Currents were measured at the end of a 1.5-s depolarizing step to 0 mV. Pooled data for KCNQ2 (□) and KCNQ3 (●) were fitted with a Hill curve (KCNQ2, IC_{50} of 1.02 μM with Hill coefficient of 2, for each concentration $n = 5$–9 cells; KCNQ3, IC_{50} of 15.7 μM and a Hill coefficient of 1.6, for each concentration $n = 6$ cells).

cells (~30%, 5 of 12 cells) (Fig. 5A). A similar rebound phenomenon was observed with the sAHP previously (Shah et al., 2006), and we did not investigate it further. Increasing the concentration of UCL2077 from 3 to 10 μM did not significantly increase the level of block in cells in which both concentrations were tested (Fig. 5C). In a subset of cells, we were able to construct dose-response curves with either 0.3 to 3 μM or 0.3 to 10 μM UCL2077. We fitted each cell's concentration-response data to a logistic function and obtained an average IC_{50} value of 1.1 $\pm$ 0.1 μM (n_H = 2.4 $\pm$ 0.4, n = 6).

The smaller block of KCNQ3 than KCNQ2 at depolarized potentials in the initial experiments suggested that UCL2077 might have a lower affinity for KCNQ3 channels. We measured the dose-response curve for KCNQ3 channels from 0.3 to 10 μM. Because of solubility issues with UCL2077, we could not use concentrations higher than 10 μM (Shah et al., 2006). Consistent with the hypothesis that UCL2077 blocks KCNQ3 channels with a lower affinity than KCNQ2 channels, we found that UCL2077 inhibited KCNQ3 currents with an IC_{50} of 16.3 $\pm$ 2.8 μM (n_H = 2, n = 6) (Fig. 5B).

UCL2077 Has Intermediate Effects on KCNQ2/3 Heteromers. We next tested the effects of UCL2077 on KCNQ2/3 heteromeric channels expressed in HEK293T cells. We hypothesized that one of three possibilities would occur: 1) the presence of KCNQ2 would dominate and KCNQ2/3 currents would be reduced by UCL2077 to a similar extent as KCNQ2 homomers; 2) the presence of KCNQ3 would dominate, and KCNQ2/3 currents would be mostly insensitive to UCL2077; or 3) KCNQ2/3 channels would exhibit an intermediate profile.

Consistent with previous studies (Wang et al., 1998; Selyanko et al., 2001), we observed that cells coexpressing KCNQ2 and KCNQ3 channels exhibited larger currents than cells expressing KCNQ2 or KCNQ3 alone. By comparing the size of the KCNQ2/3 heteromeric channel currents in the presence and absence of 3 μM UCL2077 (Fig. 6A), we found that UCL2077 inhibits KCNQ2/3 channels 38 $\pm$ 7% at 0 mV (n = 8) (Fig. 6B). This magnitude of inhibition seen on heteromeric channels is approximately halfway between the percentage block of KCNQ2 and KCNQ3 homomers, consistent with the KCNQ2/3 channels forming a heteromeric complex (Wang et al., 1998; Shapiro et al., 2000). Next, we examined the effects of 3 μM UCL2077 on the G-V relationship of KCNQ2/3 heteromeric channels. Similar to KCNQ3, UCL2077 shifted the KCNQ2/3 channels voltage-dependence leftward, although the magnitude of the shift was considerably smaller ($V_{0.5}$ = $-$26.5 $\pm$ 2.3 mV before and $-$29.9 $\pm$ 2.7 mV after UCL2077, n = 8, $p < 0.05$) (Fig. 6C). We could not observe a clear facilitation of KCNQ2/3 currents at any membrane potential, most likely because of the smaller G-V shift. However, we did find that the effects of UCL2077 on

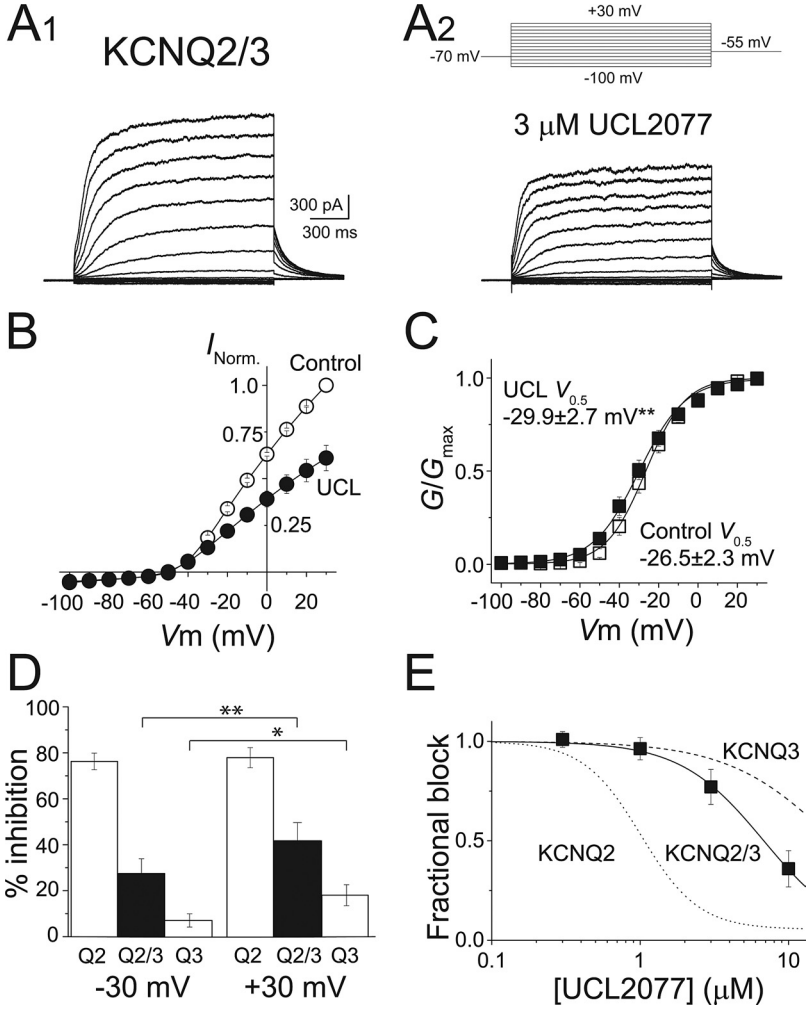

Fig. 6. Intermediate effects of UCL2077 on KCNQ2/3 currents. A, representative currents elicited by depolarization from $-$100 to +30 mV in 10-mV steps as shown (top, A_2), before (A_1) and after (A_2) application of 3 μM UCL2077. Current-to-voltage (B) and conductance-to-voltage (C) relationships of KCNQ2/3 channels in the presence (●) and absence (○) of 3 μM UCL2077 (n = 8). D, graph summarizing the inhibition by 3 μM UCL2077 of KCNQ2, KCNQ2/3, and KCNQ3 channels at test potentials of $-$30 and +30 mV. *, $p < 0.05$; **, $p < 0.01$. E, dose-response curve for UCL2077 inhibition of KCNQ2/3 currents (■, n = 5) measured at the end of a 1.5-s depolarizing step to 0 mV. Fitting the data with a Hill curve gave the following values: KCNQ2/3, IC_{50} of 6.8 μM with Hill coefficient of 1.5. Fitted Hill curves for KCNQ2 (dotted line) and KCNQ3 (dashed line) are shown for comparison.

KCNQ2/3 are voltage-dependent, with greater block occurring at +30 mV than at −30 mV (Fig. 6D). In addition, we found that the affinity of UCL2077 for KCNQ2/3 channels (7.3 ± 1.7 μM, $n = 5$; 0 mV) is in between the IC_{50} values of KCNQ2 and KCNQ3 homomers (Fig. 6E). Together, our data suggest that UCL2077 most likely acts on each subunit of the KCNQ2/3 heteromer independently, such that the heteromeric channel's response to UCL2077 is intermediate between the extremes of KCNQ2 and KCNQ3 homomers.

Discussion

UCL2077 was discovered as a small-molecule blocker of the sAHP in brain slices, but the molecular identity of its target was unknown. Here, we show that UCL2077 acts on KCNQ channels in heterologous cells. The fact that UCL2077 inhibits some KCNQ channels should not be completely surprising considering that its chemical structure is similar to XE-991, a potent nonselective KCNQ channel inhibitor (Wang et al., 1998; Zaczek et al., 1998). Both XE-991 and UCL2077 have a hydrophobic aromatic region and a positively charged hydrophilic domain but differ in that UCL2077 is less sterically hindered than XE-991. More specifically, XE-991 contains a large multiaryl moiety connected to two aromatic amines that would be positively charged at physiological pH. UCL2077 has a multiaryl moiety connected to an aromatic amine through an additional primary amine. Both amines are positively charged at physiological pH.

A major finding of our work is that UCL2077 inhibits KCNQ channels in a subtype-selective manner (Fig. 2). We found that UCL2077 robustly and potently inhibits homomeric KCNQ1 and KCNQ2 channels in heterologous cells whereas it has a bimodal effect on KCNQ3. UCL2077, at the concentrations tested in this study, has small inhibitory effects on homomeric KCNQ4 channels, whereas it causes small facilitation of homomeric KCNQ5 currents at some membrane potentials (Fig. 2). Some of these effects on KCNQ3 and KCNQ4 may be mediated through changes in the voltage-dependence of activation (Figs. 3 and 4).

The affinity of UCL2077 for KCNQ1 is more than 10-fold higher than for KCNQ2, the second most sensitive KCNQ channel, because 30 nM UCL2077 blocks KCNQ1 currents by 80 ± 3% at 0 mV (Supplemental Fig. S1). Inhibition of KCNQ1 by UCL2077 increases with increasing duration of the depolarization pulse, and KCNQ1 tail currents are more robustly inhibited than the steady-state KCNQ1 currents (Supplemental Fig. S1), unlike all the other KCNQ family members. Future studies are needed to examine how the mechanisms by which UCL2077 inhibits KCNQ1 and KCNQ2 channels differ.

The bimodal action of UCL2077 on KCNQ3 resembles the activity previously reported for retigabine, a KCNQ channel opener, although they belong to different classes of compounds (Tatulian et al., 2001; Schenzer et al., 2005). Retigabine potentiates KCNQ channel activity by shifting their voltage dependence to more hyperpolarized membrane potentials, but it also inhibits KCNQ mediated currents at membrane potentials greater than −10 mV (Tatulian et al., 2001). A later study showed the leftward voltage-dependence shift induced by retigabine in KCNQ2 channels is dependent on a specific tryptophan residue (Schenzer et al., 2005; Wuttke et al., 2005). We found that the facilitating effect of UCL2077 on KCNQ3 depends on the analogous tryptophan Trp265, because substituting leucine for Trp265 eliminated the facilitatory action of UCL2077 on KCNQ3 (Fig. 5). We hypothesize that the potentiating effect of UCL2077 on KCNQ3 might be due to stabilization of the central pore cavity during activation of KCNQ3, as has been proposed previously for retigabine (Schenzer et al., 2005; Wuttke et al., 2005). The mechanism by which retigabine, UCL2077, and XE-991 inhibit KCNQ channels is unknown.

The identification of UCL2077 as a potent subtype-selective blocker of KCNQ channels can greatly facilitate our understanding of KCNQ channel function in the nervous system. In particular, it may clarify which KCNQ subunits contribute to specific KCNQ-mediated conductances. For example, the molecular composition of the M-current may or may not vary by cell-type and developmental age in the hippocampus. Hippocampal dentate granule cells exclusively express KCNQ2 and KCNQ3 subunits, whereas neighboring CA1 and CA3 pyramidal neurons additionally express KCNQ5 (Cooper et al., 2001; Tzingounis et al., 2010). Complicating the picture, each channel is also developmentally regulated (Geiger et al., 2006; Winter et al., 2006; Safiulina et al., 2008). UCL2077 could also be used to distinguish the role of KCNQ1 and KCNQ4 in the auditory system, in which they are coexpressed in the cochlea (Jentsch, 2000).

UCL2077 is known to block the calcium-activated sAHP in multiple brain regions. However, the channels mediating the sAHP have not been definitively identified. In hippocampal slices, 10 μM UCL2077 inhibits ~45% of the sAHP, 3 μM blocks ~16%, and concentrations lower than 3 μM have little if any effect (Shah et al., 2006; K. Kim and A. Tzingounis, unpublished data). We have reported that KCNQ channels might partly mediate the sAHP in hippocampus. The extent by which UCL2077 inhibits the sAHP is consistent with our hypothesis that KCNQ3 and KCNQ2/3 channels contribute to the sAHP (see Figs. 5C and 6E) (Tzingounis and Nicoll, 2008; Tzingounis et al., 2010). However, we cannot definitely conclude which subunits mediate the sAHP based on the data in this work alone. Our findings do not preclude the possibility that another potassium channel family is also sensitive to UCL2077 and mediates the sAHP. In addition, we cannot determine the IC_{50} of UCL2077 block of the sAHP because UCL2077 is not soluble at concentrations greater than 10 μM.

Recent work has suggested that the molecular composition of the sAHP may vary by cell type (Tzingounis and Nicoll, 2008; Tzingounis et al., 2010). Likewise, UCL2077 inhibition of the sAHP varies between different brain areas and also depends on the calcium source (Shah et al., 2006; Zhang et al., 2009; Lee et al., 2010), perhaps suggesting that different combinations of KCNQ subunits and/or additional potassium channel families mediate the sAHP. Future studies using KCNQ subunit knockout mice are required to determine the absolute specificity of UCL2077 in the forebrain and to tease apart the specific KCNQ subunits contributing to the sAHP.

Acknowledgments

We thank Rima Pant for maintaining cell cultures, Drs. Dennis Wright and James Chambers for advice on the chemical structure of XE-991 and UCL2077, and Dr. Karen Menuz for comments on the manuscript.

References

Biervert C, Schroeder BC, Kubisch C, Berkovic SF, Propping P, Jentsch TJ, and Steinlein OK (1998) A potassium channel mutation in neonatal human epilepsy. *Science* **279:**403–406.

Charlier C, Singh NA, Ryan SG, Lewis TB, Reus BE, Leach RJ, and Leppert M (1998) A pore mutation in a novel KQT-like potassium channel gene in an idiopathic epilepsy family. *Nat Genet* **18:**53–55.

Cooper EC, Harrington E, Jan YN, and Jan LY (2001) M channel KCNQ2 subunits are localized to key sites for control of neuronal network oscillations and synchronization in mouse brain. *J Neurosci* **21:**9529–9540.

Geiger J, Weber YG, Landwehrmeyer B, Sommer C, and Lerche H (2006) Immunohistochemical analysis of KCNQ3 potassium channels in mouse brain. *Neurosci Lett* **400:**101–104.

Goldman AM, Glasscock E, Yoo J, Chen TT, Klassen TL, and Noebels JL (2009) Arrhythmia in heart and brain: KCNQ1 mutations link epilepsy and sudden unexplained death. *Sci Transl Med* **1:**2ra6.

Jentsch TJ (2000) Neuronal KCNQ potassium channels: physiology and role in disease. *Nat Rev Neurosci* **1:**21–30.

Kharkovets T, Dedek K, Maier H, Schweizer M, Khimich D, Nouvian R, Vardanyan V, Leuwer R, Moser T, and Jentsch TJ (2006) Mice with altered KCNQ4 K+ channels implicate sensory outer hair cells in human progressive deafness. *EMBO J* **25:**642–652.

Kubisch C, Schroeder BC, Friedrich T, Lütjohann B, El-Amraoui A, Marlin S, Petit C, and Jentsch TJ (1999) KCNQ4, a novel potassium channel expressed in sensory outer hair cells, is mutated in dominant deafness. *Cell* **96:**437–446.

Lee K, Duan W, Sneyd J, and Herbison AE (2010) Two slow calcium-activated afterhyperpolarization currents control burst firing dynamics in gonadotropin-releasing hormone neurons. *J Neurosci* **30:**6214–6224.

Lerche C, Scherer CR, Seebohm G, Derst C, Wei AD, Busch AE, and Steinmeyer K (2000) Molecular cloning and functional expression of KCNQ5, a potassium channel subunit that may contribute to neuronal M-current diversity. *J Biol Chem* **275:**22395–22400.

Maljevic S, Wuttke TV, and Lerche H (2008) Nervous system KV7 disorders: breakdown of a subthreshold brake. *J Physiol* **586:**1791–1801.

Maljevic S, Wuttke TV, Seebohm G, and Lerche H (2010) KV7 channelopathies. *Pflugers Arch* **460:**277–288.

Nicoll RA (1988) The coupling of neurotransmitter receptors to ion channels in the brain. *Science* **241:**545–551.

Otto JF, Yang Y, Frankel WN, White HS, and Wilcox KS (2006) A spontaneous mutation involving Kcnq2 (Kv7.2) reduces M-current density and spike frequency adaptation in mouse CA1 neurons. *J Neurosci* **26:**2053–2059.

Peters HC, Hu H, Pongs O, Storm JF, and Isbrandt D (2005) Conditional transgenic suppression of M channels in mouse brain reveals functions in neuronal excitability, resonance and behavior. *Nat Neurosci* **8:**51–60.

Safiulina VF, Zacchi P, Taglialatela M, Yaari Y, and Cherubini E (2008) Low expression of Kv7/M channels facilitates intrinsic and network bursting in the developing rat hippocampus. *J Physiol* **586:**5437–5453.

Schenzer A, Friedrich T, Pusch M, Saftig P, Jentsch TJ, Grötzinger J, and Schwake M (2005) Molecular determinants of KCNQ (Kv7) K+ channel sensitivity to the anticonvulsant retigabine. *J Neurosci* **25:**5051–5060.

Schroeder BC, Hechenberger M, Weinreich F, Kubisch C, and Jentsch TJ (2000) KCNQ5, a novel potassium channel broadly expressed in brain, mediates M-type currents. *J Biol Chem* **275:**24089–24095.

Selyanko AA, Hadley JK, and Brown DA (2001) Properties of single M-type KCNQ2/KCNQ3 potassium channels expressed in mammalian cells. *J Physiol* **534:**15–24.

Shah MM, Javadzadeh-Tabatabaie M, Benton DC, Ganellin CR, and Haylett DG (2006) Enhancement of hippocampal pyramidal cell excitability by the novel selective slow-afterhyperpolarization channel blocker 3-(triphenylmethylaminomethyl)pyridine (UCL2077). *Mol Pharmacol* **70:**1494–1502.

Shapiro MS, Roche JP, Kaftan EJ, Cruzblanca H, Mackie K, and Hille B (2000) Reconstitution of muscarinic modulation of the KCNQ2/KCNQ3 K(+) channels that underlie the neuronal M current. *J Neurosci* **20:**1710–1721.

Singh NA, Charlier C, Stauffer D, DuPont BR, Leach RJ, Melis R, Ronen GM, Bjerre I, Quattlebaum T, Murphy JV, et al. (1998) A novel potassium channel gene, KCNQ2, is mutated in an inherited epilepsy of newborns. *Nat Genet* **18:**25–29.

Singh NA, Otto JF, Dahle EJ, Pappas C, Leslie JD, Vilaythong A, Noebels JL, White HS, Wilcox KS, and Leppert MF (2008) Mouse models of human KCNQ2 and KCNQ3 mutations for benign familial neonatal convulsions show seizures and neuronal plasticity without synaptic reorganization. *J Physiol* **586:**3405–3423.

Tatulian L, Delmas P, Abogadie FC, and Brown DA (2001) Activation of expressed KCNQ potassium currents and native neuronal M-type potassium currents by the anti-convulsant drug retigabine. *J Neurosci* **21:**5535–5545.

Tzingounis AV, Heidenreich M, Kharkovets T, Spitzmaul G, Jensen HS, Nicoll RA, and Jentsch TJ (2010) The KCNQ5 potassium channel mediates a component of the afterhyperpolarization current in mouse hippocampus. *Proc Natl Acad Sci USA* **107:**10232–10237.

Tzingounis AV and Nicoll RA (2008) Contribution of KCNQ2 and KCNQ3 to the medium and slow afterhyperpolarization currents. *Proc Natl Acad Sci USA* **105:**19974–19979.

van den Berg MH, Wilde AA, Robles de Medina EO, Meyer H, Geelen JL, Jongbloed RJ, Wellens HJ, and Geraedts JP (1997) The long QT syndrome: a novel missense mutation in the S6 region of the KVLQT1 gene. *Hum Genet* **100:**356–361.

Wang HS, Pan Z, Shi W, Brown BS, Wymore RS, Cohen IS, Dixon JE, and McKinnon D (1998) KCNQ2 and KCNQ3 potassium channel subunits: molecular correlates of the M-channel. *Science* **282:**1890–1893.

Wen H and Levitan IB (2002) Calmodulin is an auxiliary subunit of KCNQ2/3 potassium channels. *J Neurosci* **22:**7991–8001.

Winter H, Braig C, Zimmermann U, Geisler HS, Fränzer JT, Weber T, Ley M, Engel J, Knirsch M, Bauer K, et al. (2006) Thyroid hormone receptors TRalpha1 and TRbeta differentially regulate gene expression of Kcnq4 and prestin during final differentiation of outer hair cells. *J Cell Sci* **119:**2975–2984.

Wollnik B, Schroeder BC, Kubisch C, Esperer HD, Wieacker P, and Jentsch TJ (1997) Pathophysiological mechanisms of dominant and recessive KVLQT1 K^+ channel mutations found in inherited cardiac arrhythmias. *Hum Mol Genet* **6:**1943–1949.

Wua YJ and Dworetzky SI (2005) Recent developments on KCNQ potassium channel openers. *Curr Med Chem* **12:**453–460.

Wuttke TV, Seebohm G, Bail S, Maljevic S, and Lerche H (2005) The new anticonvulsant retigabine favors voltage-dependent opening of the Kv7.2 (KCNQ2) channel by binding to its activation gate. *Mol Pharmacol* **67:**1009–1017.

Zaczek R, Chorvat RJ, Saye JA, Pierdomenico ME, Maciag CM, Logue AR, Fisher BN, Rominger DH, and Earl RA (1998) Two new potent neurotransmitter release enhancers, 10,10-bis(4-pyridinylmethyl)-9(10H)-anthracenone and 10,10-bis(2-fluoro-4-pyridinylmethyl)-9(10H)-anthracenone: comparison to linopirdine. *J Pharmacol Exp Ther* **285:**724–730.

Zaika O, Hernandez CC, Bal M, Tolstykh GP, and Shapiro MS (2008) Determinants within the turret and pore-loop domains of KCNQ3 K+ channels governing functional activity. *Biophys J* **95:**5121–5137.

Zhang L, Renaud LP, and Kolaj M (2009) Properties of a T-type Ca^{2+}channel-activated slow afterhyperpolarization in thalamic paraventricular nucleus and other thalamic midline neurons. *J Neurophysiol* **101:**2741–2750.

Zhang L, Weiner JL, Valiante TA, Velumian AA, Watson PL, Jahromi SS, Schertzer S, Pennefather P, and Carlen PL (1994) Whole-cell recording of the Ca(2+)-dependent slow afterhyperpolarization in hippocampal neurones: effects of internally applied anions. *Pflugers Arch* **426:**247–253.

Address correspondence to: Dr. Anastassios V. Tzingounis, Department of Physiology and Neurobiology, University of Connecticut, Storrs, CT 06269. E-mail: anastasios.tzingounis@uconn.edu